

The Impacts of Hg(II) Tightly Binding on the Alzheimer's Tau Construct R3: Misfolding and Aggregation

Dan-Jing Yang,[1,2] Shuo Shi,[1] Tian-Ming Yao,*[1] and Liang-Nian Ji[1]

[1]Department of Chemistry, Tongji University, Shanghai 200092, P. R. China

[2]School of Medicine, Tongji University, Shanghai 200092, P. R. China

Received May 10, 2011; E-mail: tmyao@tongji.edu.cn

Mercury, a known neurotoxin, is increasingly believed to be relevant to trigger the pathological positive feedback circle of Alzheimer's disease (AD). In this study, we originally set out to determine the possible mechanisms for Hg(II)-stimulated fibrillation of R3, which is pivotal to the biochemical properties of full tau protein. In an isothermal titration calorimetry experiment, we demonstrate that R3 shows high affinity to Hg(II), and it yields two types of coordination intermediates in the Hg(II)–R3 binding process. The exceptionally large magnitude of heat release suggests that the most possible coordinating site is the thiol group of cysteine residue (Cys322). By circular dichroism spectrum, we reveal that the coordination of Hg(II) significantly alters the conformation of natively unstructured R3, specifically from random coil to β-turn structure. Furthermore, we find that the tight binding of Hg(II) exerts a pronounced acceleration of the heparin-induced aggregation of R3, giving relatively more R3 filaments, by ThS fluorescence assay and electron microscopy. This investigation could help us to understand the detailed mechanism of misfolding development and self-aggregation of the tau protein from a toxicological perspective of metal ion to AD.

Alzheimer's disease (AD) is the most common neurodegenerative disease in the elderly.[1,2] It is characterized by the presence of both intraneuronal protein clusters composed of paired helical filaments (PHFs) of tau protein [neurofibrillary tangles (NFTs)],[3] and extracellular protein aggregates of β-amyloid peptide [senile plaques (SPs)].[4] The cause of AD is yet unknown. The longitudinal clinicopathologic cohort study, using summary measures of amyloid load, shows no correlation between amyloid load and clinical AD and global cognitive function. This finding suggests that the effect of amyloid deposition on clinical disease is mediated by NFTs.[5] Furthermore, the clearance of amyloid plaques does not prevent progressive neurodegeneration.[6] Therefore, the question of how and why tau becomes insoluble and aggregates into PHFs is one of the most key issues in molecular AD research.

The original studies of tau protein from brain tissue have already revealed its unusual features that tau is devoid of secondary or tertiary structure and retains its biological function even after harsh treatment (boiling and acid).[7] However, in AD, tau can accumulate in filamentous forms that demonstrate a remarkable degree of order. It's reported that the conformational change is one of the earliest alterations of tau in AD[8] and widely believed to be the central event in tau aggregation. Considerable attention is presently focused on tau protein misfolding–aggregation and on the starting points of both these processes as a tool to elucidate the molecular and biochemical basis of the conformational disorders.[9–11] However, the question about the factors that trigger the changes of sequence in the earlier stages of folding is still not well answered.

The sporadic nature of AD argues for an environmental link that may drive AD pathogenesis.[2] Although the mechanism by which tau protein aggregates is not fully understood, increasing evidences show that metals play important roles in precipitation and toxicity of this protein. There have been results indicating that Ca^{2+} and Mg^{2+} could selectively induce the formation of PHF–tau aggregation,[12] whereas Al^{3+},[13] Cu^{2+},[14] Fe^{2+}/Fe^{3+},[15,16] Zn^{2+},[17] and Cd^{2+},[18] could bind to tau. Tau was also found capable of adventitious binding of copper and iron in a redox-competent manner.[15,16]

Mercury, known as a neurotoxin,[19] is increasingly believed to be relevant to trigger the pathological positive feedback circle of AD.[20,21] It seems that mercury is absorbed or accumulated in degenerative AD brain more readily than those of controls.[19] Hg levels have been reported to be elevated in some brain regions in patients with AD.[20,22,23] Low levels of inorganic mercury are able to cause AD-typical nerve cell deteriorations in vitro and in animal experiments.[20,22] However, the effect of mercury on the fibrillation of tau protein is yet to be determined.

To evaluate the potential role of mercury in the folding of tau protein during the development of NFTs, a typical hallmark of AD, we systematically investigate the interaction between mercury and tau construct R3 (corresponding to the third repeat unit of microtubule-binding domain, residues 306–336: VQIVY KPVDL SKVTS KCGSL GNIHH KPGGG Q, according to the longest tau protein) by several biophysical techniques, such as isothermal titration calorimetry (ITC), circular dichroism spectrum (CD), ThS fluorescence assay, and electron microscopy (EM). The assembling and structural features of microtubule-binding domain of tau are most important, because tau–microtubule interaction is based on the "repeat-domain,"[24] including three to four pseudorepeats of $\approx$31 residues, which also forms the core of PHFs.[25] Among the four pseudorepeats, repeat unit R3 is believed to be pivotal to the biochemical properties of full tau protein, because: 1) R3

Published on the web November 29, 2011; doi:10.1246/bcsj.20110133

exhibits the highest self-assembly speed and the smallest critical concentration in filament formation processes, and the aggregation of the three-repeat tau-isoforms is R3-driven;[26] 2) the hexapeptide ^{306}VQIVYK^{311} which is able to initiate the tau aggregation process locates at the N-terminal of R3.[27] Threfore, we hereby carry out new experiments to investigate the impacts of Hg(II) on tau filament formation by using R3 peptide. The investigation is ultimately aimed to identify the toxicity of Hg(II) with respect to the ever elusive initial factor(s) that triggers the development of tau aggregation.

Results and Discussion

Thermodynamic Properties for the Binding of Hg(II) to R3: ITC Measurement. To characterize the thermodynamic properties of Hg(II) binding to R3, isothermal titration calorimetry (ITC) was carried out. In Figure 1A, each heat pulse corresponded to an injection of Hg(II) ions into the peptide solution. The raw data indicated exothermic interactions, based on the negative values observed for the peaks. The heat effects associated with the dilution of reactants was estimated by titrating Hg(II) ion into buffer solution without R3, and titrating blank buffer into R3/Tris-HCl buffer solution under the same conditions. The heats of dilution were subtracted prior to analysis. Then the data were integrated to generate the binding isotherm in which the kilocalories per mole of injected metal ions were plotted against the molar ratios of metal ions to peptide, as shown in Figure 1B.

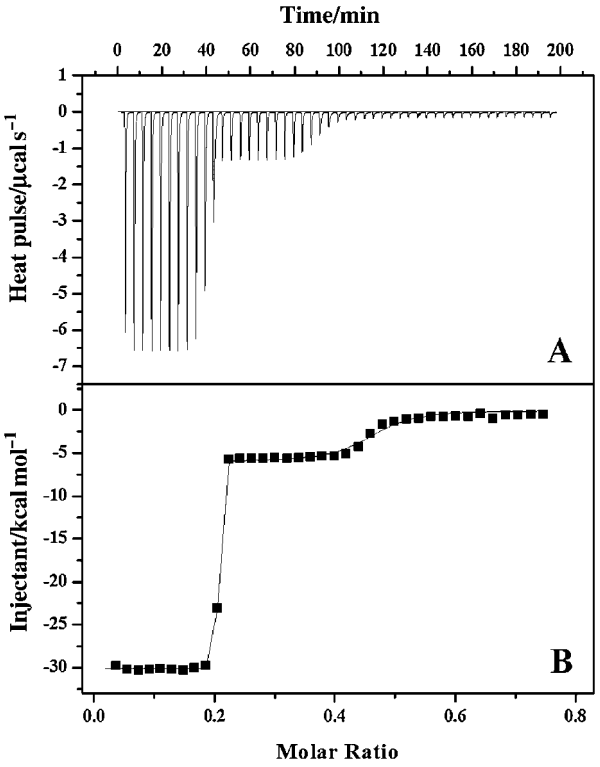

Figure 1. (A) ITC raw data for titration of $HgCl_2$ (1021 μM) into R3 (306 μM) in 50 mM Tris-HCl buffer (pH 7.50) at 37 °C; Cell volume: 1.43 mL; Stirring speed: 290 rpm. (B) The integrated heat data, together with the fit of the data obtained with a two sets of binding sites model, titration of $HgCl_2$ (1021 μM) into R3 (306 μM).

Usually, ITC measures heat generated upon binding, and provides in a single experiment the values of n (number of binding sites), ΔH (reaction enthalpy change in cal mol^{-1}), and K_b (binding constant). The reaction entropy ΔS is calculated using the equations $\Delta G = -RT \ln K_b$ ($R = 1.9872$ cal mol^{-1} K^{-1}, $T = 298.15$ K) and $\Delta G = \Delta H - T\Delta S$.

For the titration of Hg(II), the best fit was obtained using the two sets of binding sites model, with the numbers of binding sites, $n_1 = 0.21 \pm 0.001$, $n_2 = 0.258 \pm 0.01$. On the basis of the coordination chemistry of Hg^{2+} (d^{10}), we postulate that Hg(II) binds to R3 with a two-step binding process.

At the beginning of titration, because of the relatively higher concentrations of R3 than Hg(II), the formation of the first product would resemble a tetrahedral, four-coordinate complex of HgL_4, corresponding to the molar ratio of Hg(II) to R3, $n_1 = 0.21 \pm 0.001$ (L represents tau constructs R3):

$$4L + Hg^{2+} \rightleftharpoons HgL_4 \quad (1)$$
$$K_{b1} = 1.16 \times 10^{21};\ \Delta H_1 = -30.12 \text{ kcal mol}^{-1};$$
$$\Delta S_1 = -0.71 \text{ cal mol}^{-1} \text{ K}^{-1}$$

The binding enthalpy primarily reflects the strength of the interactions of the ligand with the target protein relative to those existing with the solvent.[28] Here the very large magnitude of heat release is most likely to be an indication of the formation of metal–sulfur coordination bond(s), probably between the Hg(II) ion and the thiol sulfur atom of cysteine (Cys322) on the peptide chain.[29] The tendency of ligands to coordinate with Hg(II) depends on the donor atom, and this decreases in the following order: S > N > O.[29,30] Because each atom in Hg(II)–S bond can polarize the other and the mutual polarizability between S and Hg(II) is higher than that of N or O,[30] Cys322, the single free sulfhydryl-containing amino acid in R3 monomer, preferentially coordinates to Hg(II). And this interaction is usually strongly exothermic.[29]

With the titration of additional Hg(II) into solution, the newly introduced Hg(II) acquires two ligands (R3) from HgL_4 complex, and the complex recomposes to give the two-coordinate complex of HgL_2, corresponding to the molar ratio of Hg(II) to R3, $n = n_1 + n_2 = 0.47 \pm 0.01$:

$$HgL_4 + Hg^{2+} \rightleftharpoons 2HgL_2 \quad (2)$$
$$K_{b2} = 8.67 \times 10^{5};\ \Delta H_2 = -6.05 \text{ kcal mol}^{-1};$$
$$\Delta S_2 = +7.67 \text{ cal mol}^{-1} \text{ K}^{-1}$$

In this step, the coordination environment of Hg(II) changes from "four-coordinated, tetrahedral geometry" to "two-coordinated, linear geometry." However, it is simply a ligand rearrangement reaction, no additional coordination bond forms in this process. Therefore, the heat release in the second step is much smaller than that in the first step.

Combining eq 1 with eq 2, the overall reaction is,

$$2L + Hg^{2+} \rightleftharpoons HgL_2 \quad (3)$$
$$K_b = \sqrt{K_{b1} K_{b2}} = 3.17 \times 10^{13};$$
$$\Delta H = \frac{1}{2}(\Delta H_1 + \Delta H_2) = -18.08 \text{ kcal mol}^{-1};$$
$$\Delta S = \frac{1}{2}(\Delta S_1 + \Delta S_2) = +3.48 \text{ cal mol}^{-1} \text{ K}^{-1}$$

In the overall reaction, the binding affinity is enthalpically driven and characterized by slightly favorable entropy. Com-

pared with binding of Cu(II) or Zn(II) to the thiol sulfur of cysteine in tau protein, where the enthalpy value $\Delta H = -14.6$ or $-15.0\,\mathrm{kcal\,mol^{-1}}$,[14,16] the Hg(II) binding shows a very large enthalpic contribution $\Delta H = -18.08\,\mathrm{kcal\,mol^{-1}}$. Hg(II) ions are known to carry a unique property to bind thiol groups with an exceptionally high association constant, preferentially forming a stable S–Hg(II)–S bridge which is reminiscent of the physiologically occurring disulfide (S–S) bond in oxidative cellular environments. The disulfide bond formation is believed to be a very important driving force for tau aggregation.[31]

The Conformational Alteration of R3 Induced by Hg(II): CD Spectrum. Information of structural changes in proteins induced by the binding of metal ions is an essential part of the mechanism of action and regulation of biological activity. CD provides an experimentally convenient means of detecting such changes. In the absence of Hg(II) ions (Figure 2A, curve a), the CD spectrum of R3 peptide displayed a minimum at approximately 198 nm, which was consistent with a random coil structure. As the concentration of Hg(II) ion increased, a conformational transition was observed in the CD spectroscopic manifold, in which a positive signal at about 211 nm emerged. This positive signal is assigned to β-turn structure as reported by the literature.[32,33] Plots of the CD signals at 198 and 211 nm versus the molar ratios of Hg(II) to R3 (Figure 2B), clearly suggest a conformational conversion from random coil to β-turn structure, a refolding of R3 peptide chain induced by Hg(II) coordination. Such a conformational transformation is believed to be a key factor for tau aggregation.

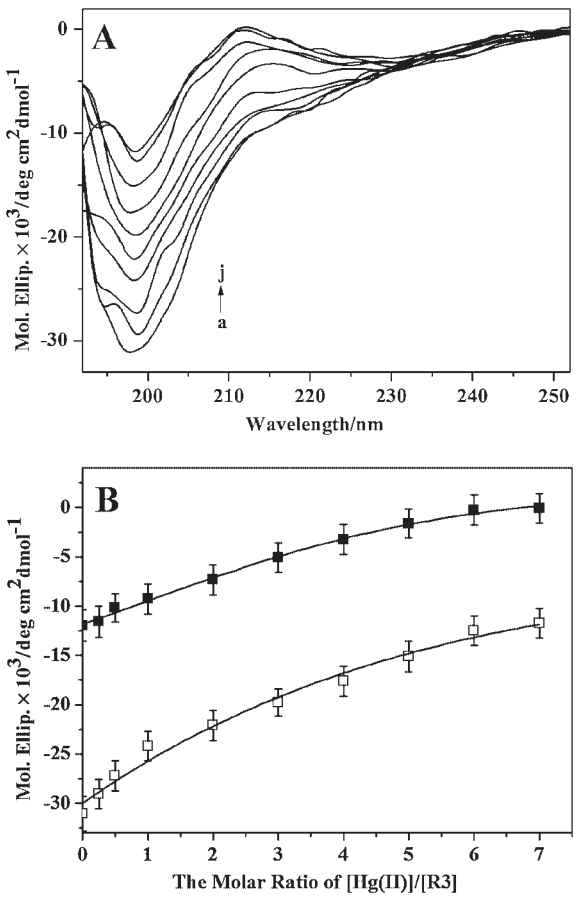

Figure 2. (A) CD spectra of R3 with different amounts of $HgCl_2$. The sample solutions are 40.00 μM R3 mixed with the molar ratio of [Hg(II)]/[R3] (from a to j): 0.00, 0.25, 0.50, 1.00, 2.00, 3.00, 4.00, 5.00, 6.00, and 7.00 in phosphate buffer (pH 7.50). (B) Plots of the CD signals at 198 nm/211 nm versus the molar ratio of $[HgCl_2]$/[R3].

Many efforts have been directed toward determining the fundamental forces involved in metalloprotein folding and structure. A simplified view of the forces influencing overall Hg(II)–R3 peptide structure suggests the involvement of two primary factors: (a) the driving force for Hg(II) coordination geometry with a particular ligand donor set (Cys322), which is proposed to be the main determinant of the uniqueness of the evolution of R3 misfolding, and (b) the supramolecular forces directing the misfolding of the polypeptide chain. Examples of these forces are: the electrostatic strike on the neighboring peptide chain resulting from the Hg(II) cation's positive charge; the hydrophobic and hydrophilic interaction around the –S–Hg(II)–S– intermolecular bridge, as well as hydrogen bonds, and so on.[34]

For this reason, the conformational conversion induced by Hg(II) ion is supposed to be an important driving force for tau aggregation, in addition to the synergistic impetus of polyanions such as heparin, which neutralizes the positive charge on some basic amino acid residues, for example, ^{306}VQIVYK^{311} at the N-end of peptide R3.[27] We are in the progress of using other physical techniques such as NMR to help identify the probable mode of conformational conversion.

The Aggregation Kinetics of R3 with Hg(II): ThS Fluorescence Assay. It has been reported that thioflavine dyes, such as ThS, can be used to quantify the filament formation in solution in real time. Thus we used this assay to monitor the kinetics and to examine Hg(II) influencing filament assembly. As shown in Figure 3A, without Hg(II), the time profile of the heparin-induced aggregation of R3 (curve a) showed a similar pattern as reported earlier.[35] With the addition of Hg(II), the ThS fluorescence intensity clearly enhanced, indicating that the heparin-induced aggregation of R3 was accelerated significantly, as illustrated from curve b to i.

It has been reported that the kinetic curves of tau fibrillization are consistent with a nucleation-dependent elongation model,[36] in which the lag phase corresponds to the nucleation phase, and the exponential part of a fibril growth (elongation) phase. To get better understanding of the effect of various concentrations of Hg(II) on R3 aggregation, kinetic parameters were determined by fitting ThS fluorescence intensity versus time to a sigmoidal equation,[16]

$$F = F_0 + (A + ct)/\{1 + \exp[k(t_m - t)]\} \quad (4)$$

Where F is the fluorescence intensity, k is the rate constant for the growth of fibrils, and t_m is the time to 50% of maximal fluorescence. The initial baseline during the lag time is described by F_0. The final baseline after the growth phase has ended is described by $A + ct$. The lag time is calculated as $t_m - 2/k$. The kinetic parameters of heparin-induced aggregation of R3 with different amounts of Hg(II), monitored by ThS fluorescence at 37 °C, are summarized in Table 1.

In the absence of Hg(II), the lag time for R3 was about 6.16 min, whereas the addition of different amounts of Hg(II) decreased the lag time in different ranges. Dimerization and

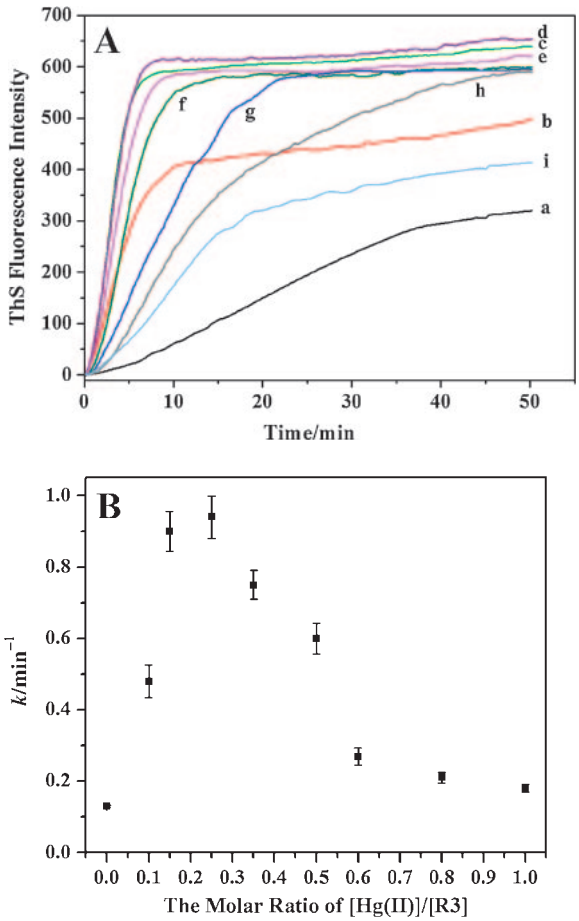

Figure 3. (A) Time-dependent profiles of R3 aggregation monitored by ThS fluorescence at 37 °C with different molar ratios of [$HgCl_2$]/[R3] (from a to i): 0.00, 0.10, 0.15, 0.25, 0.35, 0.50, 0.60, 0.80, and 1.00. R3 was adjusted to the final concentration of 15.00 μM using 50 mM Tris-HCl buffer (pH 7.50), containing 10 mM ThS dye, and different amount of metal ions. The aggregations were induced by adding heparin (final concentration was 3.80 μM) prior to fluorescence measurement. (B) The rate constants k of R3 aggregation against the molar ratios of Hg(II) to R3.

Table 1. Kinetic Parameters of Heparin-Induced Aggregation of R3 with Different Amounts of Hg(II), Monitored by ThS Fluorescence at 37 °C

[Hg(II)]/[R3]	k/min^{-1}	t_m/min	Lag time/min
0	0.13 ± 0.001	21.54 ± 0.11	6.16
0.10	0.48 ± 0.02	5.63 ± 0.07	1.46
0.15	0.90 ± 0.02	3.23 ± 0.02	1.01
0.25	0.94 ± 0.02	3.11 ± 0.02	0.98
0.35	0.75 ± 0.01	3.79 ± 0.02	1.12
0.50	0.60 ± 0.01	4.94 ± 0.03	1.61
0.60	0.27 ± 0.003	9.37 ± 0.04	1.96
0.80	0.21 ± 0.004	11.58 ± 0.16	2.06
1.00	0.18 ± 0.004	13.16 ± 0.10	2.05

nucleation are the rate-limiting steps for PHFs formation.[37] Furthermore, a dimeric tau with an intermolecular disulfide bond is presumably acting as a seed for initiation of tau polymerization.[38] The present study may be an indication that

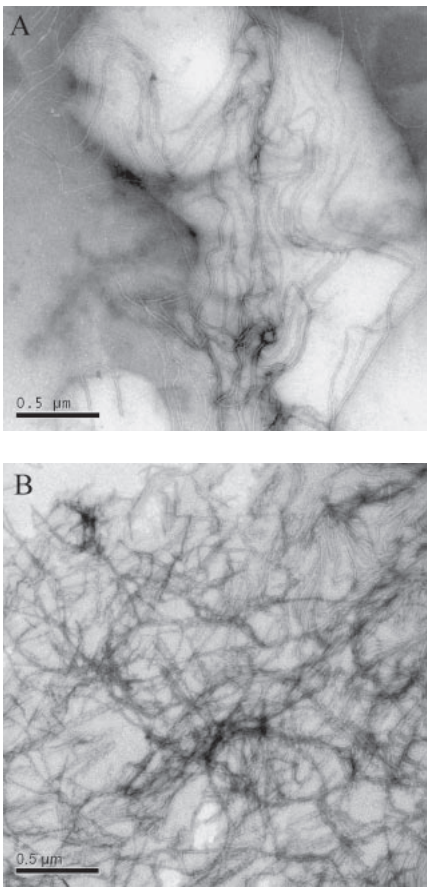

Figure 4. The EM images of the resulting R3 filaments. Aggregation of R3 (15 μM) was induced by heparin (3.80 μM) in 50 mM Tris-HCl buffer (pH 7.50). All the samples are incubated at 37 °C for 6 h. (A) without Hg(II); (B) with Hg(II) (3.80 μM).

Hg(II) is able to promote heparin-induced aggregation of R3 from a nucleation step. That is, the intermolecular linkage by S–Hg(II)–S coordination bridge facilitates the tetramerization (dimerization) and/or oligomerization of tau monomers, and the resulting tau dimers (tetramers) and/or oligomers are believed to be the basic building blocks to construct the core of filaments.

As shown in Figure 3B, the rate constants for the growth of fibrils were depicted against the molar ratios of Hg(II) to R3. It is noticed that the resulting Hg(II) dose-dependent curve is not linear, but biphasic. The maximum rate constant k is reached at approximately the molar ratio of 0.25 (Hg(II)/R3). This optimum molar ratio for promoting heparin-induced aggregation of R3 is consistent with the stoichiometry of HgL_4 complex, as we have discussed in the ITC section.

Characterization of the Morphologies of R3 Aggregation Products with Hg(II): Electron Microscopy. Conventional negative staining electron microscopy was employed to analyze the morphologies of R3 aggregation products. Figure 4 illustrated the morphologies of the aggregation products at two different conditions, (A) induced independently by heparin, (B) induced by heparin in the presence of Hg(II). Both the aggregation products are straight and long filaments, with slight helical shape, ≈13 nm in width. Similar morphology implies that Hg(II) does not change the overall molecular arrangement

within the filaments. However, a notable difference is observed in the number of filaments. That is, the filaments appear to be more abundant if Hg(II) is introduced into the system, consistent with its high ThS fluorescence signal.

Conclusion

Mercury(II), the most toxic heavy metal,[39] has been speculated to be a risk factor for the pathogenesis of AD. In this study, we originally set out to determine the possible mechanisms for Hg(II)-stimulated fibrillation of R3, the most important Alzheimer's tau construct corresponding to the third repeat of microtubule-binding domain. Here we demonstrate that R3 shows high affinity for Hg(II). In the ITC experiment, the exceptionally large magnitude of heat release suggests that the most possible coordinating site is the thiol group of cysteine residue (Cys322). Stoichiometric analysis indicates that it yields two types of coordination intermediates in the Hg(II)–R3 binding process. One is the tetrahedral coordination (HgL_4), another is the linear coordination (HgL_2, L = R3 monomer). CD spectrum reveals that the coordination of Hg(II) significantly alters the conformation of natively unstructured R3, specifically from random coil to β-turn structure. Furthermore, we find that the tight binding of Hg(II) exerts a pronounced acceleration on the heparin-induced aggregation of R3, giving relatively more R3 filaments by ThS fluorescence assay and electron microscopy. And the coordination intermediate of (HgL_4) is more toxic than that of (HgL_2) since the efficiency in promoting aggregation of the former coordination is higher than the later one.

Metal toxicity is a result of the chemical combination of metals and ligands. Based on the results by several biophysical techniques, here we believe that the impacts of Hg(II) coordination on R3 peptide chain exist on two aspects, (a) the coordination intermediates, containing the intermolecular S–Hg(II)–S bridging links, may act as effective building blocks for initiation of R3 polymerization, just mimic the physiologically occurring tau dimer, containing the intermolecular disulfide (S–S) bonds. Consequently, they dramatically enhance the R3 aggregation through the nucleation step; (b) the binding of Hg(II) can play a structural role in R3 aggregation. That is, as a central ion, Hg(II) joins four or two R3 monomers together through the S–Hg(II)–S bridging links. Concurrently, to adapt to the favorable coordination geometry, the overall R3 peptide chain is reorientated around the intermolecular S–Hg(II)–S linkage, resulting in the β-turn structure. The electrostatic interaction of Hg(II) with the surrounding peptide chain can be a trigger for conformational transition. The resulting β-turn structure strengthens the interaction between tau entities (most probably the tetramer or dimer of R3) and accordingly facilitates the polymerization through the elongation step. This investigation would help us to understand the detailed mechanism of misfolding development and self-aggregation of the tau protein from a toxicological perspective of metal ion to AD.

Experimental

Chemicals and Peptides. Heparin (average molecular weight, 6000) and ThS were obtained from Sigma Co. The R3 peptide was chemically synthesized using a solid-phase peptide synthesizer. The sample was obtained in the lyophilized form (including trifluoroacetic acid as a counter ion). The peptide was characterized by mass spectrometry and determined to be >95.0% pure by reverse-phase HPLC. Working solution of R3 was made by dilution to 1 mg mL^{-1} with 50 mM Tris-HCl buffer (pH 7.50) before use. The buffer solution contained no reducing reagent such as dithiothreitol (DTT) usually used to block the formation of disulfide bonds. All the experiments were conducted in open atmosphere. All the other chemicals were of analytical reagent grade.

ITC Measurements. ITC experiments were conducted using a MicroCal VP-ITC unit operating at 37 °C. In each experiment, 50 injections (the volume of each injection was 6 μL) of a solution containing $HgCl_2$ at a concentration of 1021 μM were titrated into a solution of R3 (306 μM) in 50 mM Tris-HCl (pH 7.50) buffer (cell volume: 1.43 mL, stirring speed: 290 rpm) using a computer-controlled 310 μL microsyringe. The pH of each solution was checked before starting the analysis. The reference cell was filled with Tris-HCl buffer. Before each experiment, the solution was degassed for 2–5 min, to eliminate air bubbles, using the ThermoVac accessory of the microcalorimeter. The first addition started after the baseline stability was achieved. To allow the system to reach equilibrium, a spacing of 240 s between each injection was applied. The feedback mode was set to "high." A control experiment was set up, titrating $HgCl_2$ solution into the buffer under the same conditions. The heat recorded after re-equilibration was due to the reaction occurring within the sample cell. All data were recorded with the software provided by the calorimeter manufacturer. Integrated heat data were fitted using a non-linear-squares minimization algorithm to a theoretical titration curve, using the MicroCal Origin software and the two sets of binding sites model.

CD Measurement. R3 solution was adjusted to 40.00 μM in phosphate buffer, with the pH adjusted to 7.50. All measurements were carried out at 25 °C with a JASCO J-810 spectrometer in a cuvette with a 10 mm path length. For each experiment, the measurement from 192 to 252 nm was repeated eight times under N_2 gas flow, and the results were summed. Then the molar ellipticity was determined after normalizing the sample concentration. The same experiment was performed at least three times using the newly prepared samples, and average values are presented in this paper.

ThS Fluorescence Assay of Aggregation. The R3 peptide was adjusted to a concentration of 15.00 μM using 50 mM Tris-HCl buffer (pH 7.50) containing 10 mM ThS dye. The aggregations were induced by adding (a) heparin (final concentration was 3.80 μM); (b) $HgCl_2$ (final concentration was different) and then heparin (final concentration was 3.80 μM) to the solution, and mixing immediately with a pipette prior to fluorescence measurement. The time-dependent fluorescence at 37 °C was monitored on a LS-55 luminescence spectrometer instrument (Perkin-Elmer) with a 2 mm quartz cell with excitation at 440 nm and emission at 500 nm. The excitation and emission slit width were both 10 nm. The background fluorescence of the sample was subtracted when needed. For each curve of time-dependent ThS fluorescence, the measurement was performed three times and averaged.

EM Measurement. R3 (15.00 μM) was mixed with (i) 3.80 μM heparin, (ii) 3.80 μM heparin, and 3.80 μM $HgCl_2$ in 50 mM Tris-HCl (pH 7.50). The solution was then incubated at 37 °C for 6 h. For negative-staining EM, 600-mesh copper grids were used. A drop of peptide solution and a drop of 2% uranylacetate were placed on the grids. After 2 min, excess fluid was removed from the grids. Negative-staining EM was performed using an electron microscope (JEOL JSM-1200EX II) operated at 80 kV.

This work was supported by the National Natural Science Foundation of China (No. 20871094 and No. 20901060), and the opening foundation of the State key laboratory of Coordination Chemistry, Nanjing University.

References

1 M. Goedert, M. G. Spillantini, *Science* **2006**, *314*, 777.
2 J. F. Wu, Md. R. Basha, N. H. Zawia, *J. Mol. Neurosci.* **2008**, *34*, 1.
3 E. Mandelkow, *Nature* **1999**, *402*, 588.
4 M. C. Montalto, G. Farrar, C. T. Hehir, *Ann. N.Y. Acad. Sci.* **2007**, *1097*, 239.
5 D. A. Bennett, J. A. Schneider, R. S. Wilson, J. L. Bienias, S. E. Arnold, *Arch. Neurol.* **2004**, *61*, 378.
6 C. Holmes, D. Boche, D. Wilkinson, G. Yadegarfar, V. Hopkins, A. Bayer, R. W. Jones, R. Bullock, S. Love, J. W. Neal, E. Zotova, J. A. R. Nicoll, *Lancet* **2008**, *372*, 216.
7 D. W. Cleveland, S.-Y. Hwo, M. W. Kirschner, *J. Mol. Biol.* **1977**, *116*, 227.
8 C. L. Weaver, M. Espinoza, Y. Kress, P. Davies, *Neurobiol. Aging* **2000**, *21*, 719.
9 K. Minoura, F. Mizushima, M. Tokimasa, S. Hiraoka, K. Tomoo, M. Sumida, T. Taniguchi, T. Ishida, *Biochem. Biophys. Res. Commun.* **2005**, *327*, 1100.
10 J. Berriman, L. C. Serpell, K. A. Oberg, A. L. Fink, M. Goedert, R. A. Crowther, *Proc. Natl. Acad. Sci. U.S.A.* **2003**, *100*, 9034.
11 S. Barghorn, P. Davies, E. Mandelkow, *Biochemistry* **2004**, *43*, 1694.
12 L.-s. Yang, H. Ksiezak-Reding, *J. Neurosci. Res.* **1999**, *55*, 36.
13 R. W. Shin, V. M. Lee, J. Q. Trojanowski, *J. Neurosci.* **1994**, *14*, 7221.
14 A. Soragni, B. Zambelli, M. D. Mukrasch, J. Biernat, S. Jeganathan, C. Griesinger, S. Ciurli, E. Mandelkow, M. Zweckstetter, *Biochemistry* **2008**, *47*, 10841.
15 L. M. Sayre, G. Perry, P. L. R. Harris, Y. Liu, K. A. Schubert, M. A. Smith, *J. Neurochem.* **2000**, *74*, 270.
16 A. Yamamoto, R.-W. Shin, K. Hasegawa, H. Naiki, H. Sato, F. Yoshimasu, T. Kitamoto, *J. Neurochem.* **2002**, *82*, 1137.
17 Z.-Y. Mo, Y.-Z. Zhu, H.-L. Zhu, J.-B. Fan, J. Chen, Y. Liang, *J. Biol. Chem.* **2009**, *284*, 34648.
18 L.-F. Jiang, T.-M. Yao, Z.-L. Zhu, C. Wang, L.-N. Ji, *Biochim. Biophys. Acta, Proteins Proteomics* **2007**, *1774*, 1414.
19 B. Bocca, G. Forte, F. Petrucci, A. Pino, F. Marchione, G. Bomboi, O. Senofonte, F. Giubilei, A. Alimonti, *Ann. Ist. Super. Sanita* **2005**, *41*, 197.
20 J. Mutter, J. Naumann, C. Sadaghiani, R. Schneider, H. Walach, *Neuroendocrinol. Lett.* **2004**, *25*, 331.
21 J. T. A. Ely, *Bull. Environ. Contam. Toxicol.* **2001**, *67*, 800.
22 J. Mutter, J. Naumann, R. Schneider, H. Walach, *Fortschr. Neurol., Psychiatr.* **2007**, *75*, 528.
23 C. M. Thompson, W. R. Markesbery, W. D. Ehmann, Y. X. Mao, D. E. Vance, *Neurotoxicology* **1988**, *9*, 1.
24 K. A. Butner, M. W. Kirschner, *J. Cell Biol.* **1991**, *115*, 717.
25 C. M. Wischik, M. Novak, P. C. Edwards, A. Klug, W. Tichelaar, R. A. Crowther, *Proc. Natl. Acad. Sci. U.S.A.* **1988**, *85*, 4884.
26 K. Tomoo, T.-M. Yao, K. Minoura, S. Hiraoka, M. Sumida, T. Taniguchi, T. Ishida, *J. Biochem.* **2005**, *138*, 413.
27 W. Li, V. M.-Y. Lee, *Biochemistry* **2006**, *45*, 15692.
28 S. Leavitt, E. Freire, *Curr. Opin. Struct. Biol.* **2001**, *11*, 560.
29 M. Ngu-Schwemlein, J. K. Merle, P. Healy, S. Schwemlein, S. Rhodes, *Thermochim. Acta* **2009**, *496*, 129.
30 *Mercury in Aquatic Ecosystems* in *Metal Metabolism in Aquatic Environments*, 1st ed., ed. by W. J. Langston, M. J. Bebianno, Chapman & Hall Ltd., **1998**, Chap. 5, p. 80.
31 S. Barghorn, E. Mandelkow, *Biochemistry* **2002**, *41*, 14885.
32 S. M. Kelly, T. J. Jess, N. C. Price, *Biochim. Biophys. Acta, Proteins Proteomics* **2005**, *1751*, 119.
33 N. J. Greenfield, *Anal. Biochem.* **1996**, *235*, 1.
34 D. L. Nelson, M. M. Cox, *Lehninger Principles of Biochemistry*, 4th ed., W. H. Freeman, New York, **2004**.
35 L.-J. Han, S. Shi, L.-F. Zheng, D.-J. Yang, T.-M. Yao, L.-N. Ji, *Bull. Chem. Soc. Jpn.* **2010**, *83*, 911.
36 P. Friedhoff, M. von Bergen, E.-M. Mandelkow, P. Davies, E. Mandelkow, *Proc. Natl. Acad. Sci. U.S.A.* **1998**, *95*, 15712.
37 E. E. Congdon, S. Kim, J. Bonchak, T. Songrug, A. Matzavinos, J. Kuret, *J. Biol. Chem.* **2008**, *283*, 13806.
38 K. Bhattacharya, K. B. Rank, D. B. Evans, S. K. Sharma, *Biochem. Biophys. Res. Commun.* **2001**, *285*, 20.
39 O. D. Tyagi, M. Mehra, *A Textbook of Environmental Chemistry*, Anmol Publications Pvt. Ltd., **2006**, p. 125.